J. Phycol. **36,** 46–58 (2000)

THE REVERSIBLE EFFECT OF FLOW ON THE MORPHOLOGY OF *CERATOCORYS HORRIDA* (PERIDINIALES, DINOPHYTA)[1]

Marnie J. Zirbel, Fabrice Veron, and Michael I. Latz[2]

Scripps Institution of Oceanography, University of California San Diego, La Jolla, California 92093-0202

Most cells experience an active and variable fluid environment, in which hydrodynamic forces can affect aspects of cell physiology including gene regulation, growth, nutrient uptake, and viability. The present study describes a rapid yet reversible change in cell morphology of the marine dinoflagellate *Ceratocorys horrida* Stein, due to fluid motion. Cells cultured under still conditions possess six large spines, each almost one cell diameter in length. When gently agitated on an orbital shaker under conditions simulating fluid motion at the sea surface due to light wind or surface chop, as determined from digital particle imaging velocimetry, population growth was inhibited and a short-spined cell type appeared that possessed a 49% mean decrease in spine length and a 53% mean decrease in cell volume. The reduction in cell size appeared to result primarily from a 39% mean decrease in vacuole size. Short-spined cells were first observed after 1 h of agitation at 20°C; after 8 to 12 d of continuous agitation, long-spined cells were no longer present. The morphological change was completely reversible; in previously agitated populations devoid of long-spined cells, cells began to revert to the long-spined morphology within 1 d after return to still conditions. During morphological reversal, spines on isolated cells grew up to 10 $\mu m \cdot d^{-1}$. In 30 d the population morphology had returned to original proportions, even though the overall population growth was zero during this time. The reversal did not occur as a result of cell division, because single-cell studies confirmed that the change occurred in the absence of cell division and much faster than the 16-d doubling time. The threshold level of agitation causing morphology change in *C. horrida* was too low to inhibit population growth in the shear-sensitive dinoflagellate *Lingulodinium polyedrum*. At the highest level of agitation tested, there was negative population growth in *C. horrida* cultures, indicating that fluid motion caused cell mortality. Small, spineless cells constituted a small percentage of the population under all conditions. Although their abundance did not change, single-cell studies and morphological characteristics suggest that the spineless cells can rapidly transform to and from other cell types. The sinking rate of individual long-spined cells in still conditions was significantly less than that of short-spined cells, even though the former are larger and have a higher cell density. These measurements demonstrate that the long spines of *C. horrida* reduce cell sinking. Shorter spines and reduced swimming would allow cells to sink away from turbulent surface conditions more rapidly. The ecological importance of the morphological change may be to avoid conditions that inhibit population growth and potentially cause cell damage.

***Key index words: Ceratocorys horrida*; dinoflagellate; growth; morphology; phytoplankton; PIV; shear; sinking; spines; turbulence**

In the aquatic environment, fluid mixing caused by wind, waves, currents, and boundary effects modifies the physical and chemical environment experienced by planktonic organisms. Vertical transport of phytoplankton changes their depth distribution (e.g. Cowles and Desiderio 1993) and alters levels of solar irradiance available for photosynthesis (Denman and Gargett 1983, Kiørboe 1993). Increased rates of nutrient uptake due to mixing can release cells from diffusion-mediated nutrient limitation and lead to enhanced growth (Pasciak and Gavis 1975, Fenchel 1988, Lazier and Mann 1989, Karp-Boss et al. 1996).

Water motion has several known physiological effects in dinoflagellates, considered one of the most shear-sensitive marine organisms (Thomas and Gibson 1990b, Berdalet and Estrada 1993, Estrada and Berdalet 1997). Laboratory studies have demonstrated that low levels of water motion inhibit the population growth of red-tide dinoflagellates (Pollingher and Zemel 1981, Thomas and Gibson 1990a, 1992) by affecting cell division (Berdalet 1992). The effect of water motion has physiological specificity, because other processes such as photosynthesis have been shown to be unaffected (Thomas et al. 1995). Laboratory studies are important in identifying mechanisms responsible for changes in natural populations, where both wind- and wave-induced turbulence may inhibit population growth (Pollingher and Zemel 1981, Tynan 1993, Rapoport and Latz 1998). High levels of fluid shear trigger flashing in bioluminescent species (Latz et al. 1994, Latz and Rohr 1999); at the most extreme, intense agitation can disrupt cell integrity (White 1976, Berdalet 1992).

The present study describes a remarkable flow-induced morphological transformation that occurs in the marine photosynthetic dinoflagellate *Ceratocorys horrida*, a cosmopolitan thecate species found in low-nutrient, warm surface waters (Graham 1942). *C. horrida* is bioluminescent, exhibiting diurnal rhythms in

[1] Received 4 May 1998. Accepted 3 November 1999.

[2] Author for reprint requests; e-mail mlatz@ucsd.edu; fax (858) 534-7313.

both spontaneous and stimulated bioluminescence (Latz and Lee 1995). The cell is distinguished by six large hypothecal spines: four projecting from the edges of the antapical plate, and single dorsal and ventral spines. The long spines are part of the thecal endoskeleton, consisting of polysaccharide deposited in flattened vesicles that lie outside a layer of cytoplasmic microtubules (Netzel and Dürr 1984). The present study examined the morphological change of *C. horrida* subjected to fluid motion simulating the action of moderate wind and waves at the sea surface. Populations were observed to contain a new short-spined form. These short-spined cells disappeared from the population upon return to still conditions. Furthermore, a small spineless cell type has been observed in still and agitated cultures. Thus, a total of three cell morphologies have been identified: long-spined, short-spined, and spineless.

The objective of the present study was to describe the phenomenon of morphological change in *C. horrida* and to test the following hypotheses regarding the effect of flow on cell morphology.

H_1: The transformation in cell morphology is due solely to fluid motion.

H_2: The transformation in morphology occurs as a result of cell division; that is, a change in morphology is evident only in daughter cells.

The results of this study suggest that the morphological transformation and its reversal in *C. horrida* may be an adaptive response to escape regions of turbulence that may cause cell damage and inhibit population growth.

MATERIALS AND METHODS

Culture and agitation conditions. Cultures of *Ceratocorys horrida* Stein, originally isolated from the Sargasso Sea during 1989 (designated 89A) (Latz and Lee 1995), were maintained under still conditions in Guillard's f/4 enriched seawater medium minus silicate at a temperature of 20 ± 1° C on a 12:12 h light–dark cycle with daytime illumination of 1000 $\mu W \cdot cm^{-2}$. The culture originated from only long-spined cells.

To observe changes in morphology due to fluid flow, cell cultures were grown on an orbital shaker for up to 40 d under identical controlled conditions of temperature and illumination. Long-spined cells at concentrations of 40 to 50 cells$\cdot mL^{-1}$ were transferred to 125-mL Pyrex flasks containing 60 mL of sterile medium. These flasks were placed on a Bellco orbital shaker, which oscillated with an orbit of 2.54 cm. Based on tests using oscillation rates of 40 through 120 rpm, a rate of 75 rpm was selected to be relatively mild while still inducing morphological transformations and inhibiting population growth. Levels of fluid velocity and shear stress in the flasks were quantified using digital particle imaging velocimetry as discussed later.

The following types of experiments were performed: (1) *control*, population grown under still conditions ($n = 4$ replicates); (2) *agitation*, population transferred from still to agitated conditions at time zero ($n = 8$); (3) *recovery*, population transferred from agitated to still conditions at time zero ($n = 4$); (4) *recovery of single isolated short-spined cells*, individual short-spined cells transferred from agitated to still conditions at time zero and maintained in individual wells ($n = 12$ cells); and (5) *recovery of spineless cells*, population of only spineless cells transferred from agitated to still conditions at time zero ($n = 8$ replicates).

Cell morphology methods. For monitoring the transition in population structure with agitation, cell concentration (cells$\cdot mL^{-1}$) for each cell type (e.g. long-spined, short-spined, and spineless) was determined periodically from 2-mL aliquots collected during the light phase. Cells with spine lengths <30 μm were considered to be short-spined and cells with no visible spines were categorized as spineless. Population growth rate was calculated as the least squares exponential regression of total cell abundance as a function of time, based on the population growth equation $N_t = N_0\, e^{\mu t}$, where N_t and N_0 are cell abundances at time t and $t = 0$, respectively, and μ is net population growth rate. The doubling time (i.e. t when $N_t/N_0 = 2$) was calculated as $t = \ln(2)/\mu$. Cell size was measured at magnifications of 50× to 126× using an ocular micrometer mounted on a Nikon SMZ-2T stereomicroscope. At least 20 cells of each morphology were measured from each sample. Cell volume was calculated according to the equation $V = 4/3\pi\ (\mathrm{ESD}/2)^3$, where ESD is the equivalent spherical diameter: $\mathrm{ESD} = (lwh)^{1/3}$, where l is cell length, w is cell width, and h is cell height.

To document changes in morphology, individual cells were imaged by SEM. Cells were isolated from populations agitated from 1 h to 4 mo, as well as from populations maintained under still conditions. Cells were fixed in an isosmotic 3% formaldehyde solution, rinsed once in filtered seawater and four times in tapwater, and then freeze-dried on gelatin-coated glass slides. The slides were coated with a 60% gold, 40% palladium alloy in a Technics Hummer sputter coater and viewed at voltages of 7 to 10 kV under a Cambridge 360 scanning electron microscope at magnifications of 750× to 1600×. Transverse and longitudinal flagella were lost during the processing for SEM.

Recovery under still conditions. To measure the recovery of populations from agitated conditions, some flasks were removed from the shaker after 10 d of continuous agitation and returned to still culture conditions. Cell morphology was monitored as previously described. To monitor the recovery of individual cells, single isolated short-spined cells from agitated cultures were transferred to individual wells of a multiwell plate and maintained at 20° C under constant illumination. The condition and size of the cells were observed by stereomicroscope with an ocular micrometer every 2 to 3 d.

Cell size measurements using laser confocal microscopy. To examine changes in the relative vacuolar and cytoplasmic volumes in cells, living cells from still and agitated culture conditions were assayed for fluorescence of luciferin, present only within the cytoplasm (Eckert and Reynolds 1967). Optical cross sections of the cells were made using a Biorad MRC1024 UV laser confocal microscope system, with argon ion laser excitation at 363 nm. Cells were viewed with a Fluor 40×/1.3 n.a. oil immersion objective using an emission filter at 455 nm with a 30 nm half bandwidth. Volume estimates for each cell were made using NIH Image software (http://rsb.info.nih.gov/nih-image/) analysis of the optical section with the largest cross-sectional area, under the assumption of a spherical cell shape. ESD was calculated from the measured cell cross-sectional area, and total cell volume was calculated from ESD as previously described. Vacuolar volume was calculated based on the cross-sectional area of the nonfluorescing region of the cell.

Measurement of sinking rates. To compare sinking rates between cell morphologies, free-falling cells within a 75-cm^2 rectangular cell culture flask were viewed at a magnification of 50× with a CCD video camera coupled to a horizontally mounted stereomicroscope. Measurements were made at a room temperature of 20 ± 0.5° C. Cells are typically motile, so two methods were used to generate nonswimming cells. Some cells were narcotized with nicotine according to the method of Kamykowski et al. (1992) by soaking 5 used cigarette filters overnight in 20 mL of filtered seawater, of which a 200-μL volume was added to 1.5 mL of cell culture containing approximately 250 cells$\cdot mL^{-1}$. Preliminary tests indicated that narcotized cells recovered swimming ability after transfer back to filtered seawater. Other cells were fixed in an isosmotic 3% formaldehyde solution. A drop of fluid containing approximately 15–20 cells was added to the surface layer of fluid in the chamber and allowed to sink approximately 3 cm (~470 cell diameters) before entering the field of view of the camera. Sinking rates were determined from

single frame analysis of the video record, based on the number of frames required for a cell to fall 0.3 mm. Although the descending cells were located approximately 1.1 cm (≥ 170 cell diameters) from the nearest chamber wall, wall effects cannot be ignored (Vogel 1994). Because the method was identical for each treatment and cell type, however, qualitative comparisons between sinking rates were relevant for the purpose of this study.

The terminal velocity for a spherical cell can be predicted from Stokes' law (Vogel 1994):

$$U_t = \frac{2r^2 g(\rho_{cell} - \rho_{seawater})}{9\,\mu_{seawater}}$$

where U_t is terminal velocity, r = ESD/2, g is acceleration due to gravity, $\rho_{seawater}$ is the density of seawater at 20°C, and $\mu_{seawater}$ is the dynamic viscosity of seawater at 20°C. It is necessary to differentiate the contributions of cell size, spine length, and cell density to terminal velocity. Because the polysaccharide thecal plates of dinoflagellates are more dense than water, it cannot be assumed *a priori* that cell density (ρ_{cell}) does not vary with cell morphology. The density of long-spined and short-spined cells was therefore measured using discontinuous sucrose gradients. Sucrose solutions ranging from 1070 to 1190 kg·m^{-3} in increments of 20 kg·m^{-3} were prepared in filtered seawater by adjusting density as measured with an electronic balance. Approximately 100 cells fixed in an isosmotic 3% formaldehyde solution and then rinsed twice in filtered seawater were layered onto the top of a 10-mL volume of each sucrose solution in 15-mL polystyrene centrifuge tubes with conical bottoms. After centrifuging at 2050 × *g* for 25 min, cell abundance was measured in a 1-mL sample withdrawn from the bottom of the tube. Mean cell density was considered 10 kg m^{-3} less than the sucrose solution which resulted in a dramatic decrease in cell abundance at the bottom of the tube, signifying that the sucrose density was greater than that of the cells. These density values were then entered into Stokes' equation to estimate the relative effect of spines on sinking rate by comparing the predicted terminal velocity of a long-spined cell with that of a smaller, less-dense short-spined cell.

Flow field measurements. Fluid motion in the shaken flasks was characterized for shaking rates of 45, 75, and 120 rpm. The velocity field was measured using digital particle imaging velocimetry (DPIV). Other methods of flow measurement, including laser Doppler velocimetry as well as heated probe, acoustic, and optical flowmeters, were not considered appropriate for the small volume and orbital motion of the shaken flasks. DPIV relies on the acquisition of sequential images of a particle-seeded fluid using video or standard photo techniques. Typically, the fluid is illuminated with a pulsed light sheet. Seeding particles are carefully chosen such that they accurately follow the fluid motion beyond the instrument resolution. Particle displacement between consecutive images or between two pulses of the light source gives a two-dimensional velocity map of the particles. This velocity map is considered to represent fluid motion, at least up to a known spatial scale.

The DPIV system used here is similar to that described by Willert and Gharib (1991) and used by Melville et al. (1998). A 2 mm thick laser sheet generated with a 5-W argon ion laser illuminated a horizontal plane through the flask, at a level of half the total fluid height. Nearly neutrally buoyant silver-coated hollow glass spheres were added to a 50-mL volume of water in the flask and were used as passive flow tracers. These particles have a density of 1150 kg·m^{-3} and an average radius of 12.7 μm. The top portion of the flask was cut off, so that a 30 Hz CCD video camera mounted above the flask could image the laser sheet. The camera was fixed to the shaker table, so the relative position between camera and flask did not change during the orbital motion of the shaker. The laser beam passed through a mechanical shutter controlled with a timer that generated sequential shutter openings in adjacent video fields. For 45 rpm, representing the threshold for morphological transformation, and 75 rpm, the standard condition used in the present study, the flask was illuminated for 4 msec with a dark interval of 10 or 16 msec, respectively, giving a δt = 14 or 20 msec, respectively; for 120 rpm, used to test for effects of high levels of agitation, the illumination time was 2 msec with a 4 msec dark interval, giving a δt = 6 msec. The very short illumination times minimized particle advection out of the laser sheet. Cross-correlation processing on sequential video images was used to retrieve the velocity and shear stress fields. The instantaneous velocity vectors **u** and **v**, and the shear stress τ, were computed on a grid of 0.53 × 0.67 mm and at a 15 Hz rate. Then, for each rpm level, 20 s of continuous data were acquired, yielding 300 velocity and shear stress maps.

There are several limitations to the use of DPIV for the measurement of the shear stress in a shaken flask. The DPIV method provides the fluid velocity, and because shear is a first order derivative of the velocity, the inherent noise in shear stress levels is greater than that of the velocity. This emphasizes the need for accurate velocity measurements. Also, the light sheet is placed at a constant depth level, while the water surface is moving up and down with forced modes traveling around the flask. This induces some vertical (out of the light sheet) motion, as well as phase coherent noise due to the surface wave. Care must be taken in choosing appropriate pulse and sampling rate to avoid aliasing. Finally, the light sheet passes through the curved wall of the glass flask, which incidentally creates a focusing lens. This prevents the entire flow from being imaged and one must then rely on the cylindrical geometry of the flow to extrapolate to the entire flask.

Unless otherwise stated, values represent means ± standard errors of the mean. Statistical analyses were performed using Statview (Abacus Concepts) and Statgraphics Plus (Manguistics) software; differences were considered significant at the 0.05 probability level.

RESULTS

When *C. horrida* was maintained in laboratory culture under still conditions, more than 80% of the cells possessed six long spines, as described by Graham (1942); these cells had an average length of 64 μm and width of 53 μm, with a mean spine length of 43 μm (Fig. 1; Table 1). Populations maintained under still conditions exhibited exponential population growth, with a doubling time of approximately 15 d (Table 2), similar to that found by Latz and Lee (1995) at 20° C.

Effect of agitation. The population growth of cultures maintained under standard agitated conditions at 75 rpm was lower than that of still controls (Fig. 2). For all replicates, population growth rate was not significantly different from zero (Table 2), indicating that the motion of the orbital shaker was sufficient to inhibit growth. Even though no net growth occurred, there was a change in the population structure from that of controls. A new short-spined cell type was observed, which consisted of reduced spine lengths and cell size compared with the long-spined cells (Fig. 1). The four antapical spines of the short-spined cells were reduced to a mean length of 22 μm, whereas the dorsal and ventral spines, if present, were no more than 20 μm in mean length. The spines of the short-spined cells were wider and more leaflike than the longer, thinner spines of the long-spined cell type.

The cell volume of short-spined cells was approximately half that of long-spined cells, and there was a 39% decrease in mean vacuole size (Table 1). Based on the spatial distribution of the fluorescence of lu-

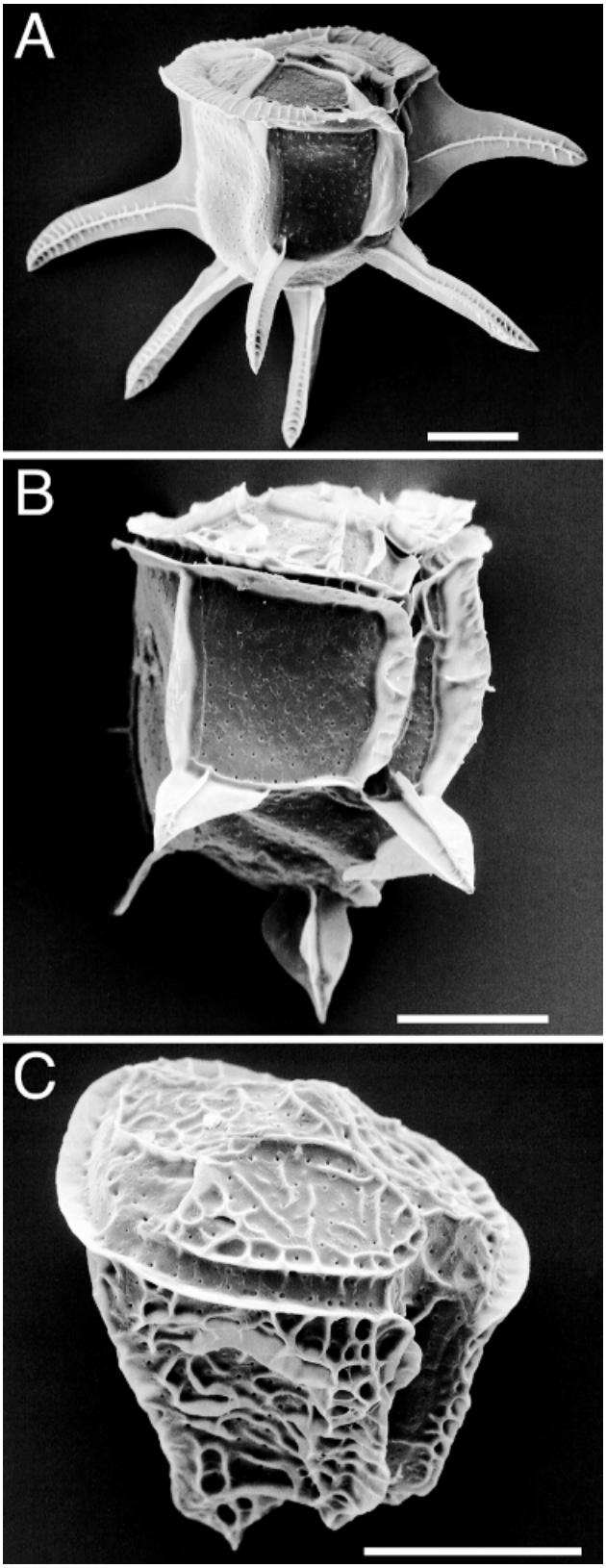

FIG. 1. Scanning electron micrographs of the different cell morphologies of *Ceratocorys horrida*. Ventral views of cells oriented with the apical portion at top; scale bars represent 20 μm. (A) Long-spined cell from a culture maintained under still conditions. (B) Short-spined cell from a culture continuously agitated at 75 rpm for 22 d. The antapical spines were much reduced in length, and broader and more leaf-like, while the dorsal and ventral spines were absent. (C) Spineless cell type observed in all cultures.

ciferin, the bioluminescence substrate which is found only in the cytoplasm (Eckert and Reynolds 1967), there was a significant decrease in the proportion of vacuolar volume to overall volume in the short-spined and spineless cells (Table 1). Long-spined cells grown in still control cultures had a mean vacuole volume comprising almost 30% of total cell volume, a proportion larger than that for many other phytoplankton cells (Costas et al. 1988). For *C. horrida* cells grown under agitation, the vacuolar volume accounted for $< 20\%$ of total cell volume. The reduction in cell size due to agitation appears therefore to be due primarily to a relative decrease in vacuolar volume.

Short-spined cells were rare in cultures maintained under still conditions. However, their relative abundance in cultures increased as a result of agitation. Short-spined cells appeared as early as 1 h after the initiation of agitation (data not shown); after 1 to 2 d of continuous agitation, more than 50% of the cells exhibited the short-spined morphology (Fig. 3). After 8 to 12 d of agitation, the proportion of short-spined cells had increased to 76.6 ± 10.8% ($n = 4$ experiments; range 63–89%) of the population, effectively replacing the long-spined cells, which decreased to only 3.9 ± 7.9% (range 0–16%) of the population. After 12 d, the population structure of the agitated cultures, which were monitored as long as 30 d, did not change.

The short-spined cells may have originated from transformation of long-spined cells. The exponential rate of decrease in abundance of long-spined cells ($\mu = -0.225 \pm 0.067$ d^{-1}, $n = 5$ experiments) was opposite that of the increase in abundance of short-spined cells ($\mu = 0.124 \pm 0.027$ d^{-1}). The absolute values of these growth rates were not significantly different ($t = 1.397$, df = 8, $P = 0.20$), suggesting that long-spined cells were transforming into short-spined cells in the absence of cell division. During this time, the change in abundance of spineless cells was not significantly different from zero ($t = 1.289$, df = 4, $P = 0.27$). Morphological data also supported the hypothesis that long-spined cells transformed into short-spined forms. After only 4 h of agitation, there was a significant 37% decrease in the mean cell volume of long-spined cells remaining ($t = 3.295$, df = 20, $P = 0.004$), due to a significant decrease in mean cell length ($t = 5.832$, df = 20, $P < 0.0001$) with only a slight change in mean cell width ($t = 1.966$, df = 20, $P = 0.06$). Few long-spined cells were present after 12 d of agitation.

Following transformation, the mean cell size (volume, ESD, length, width) of short-spined cells did not change even after 4 mo of continuous agitation (volume: $F = 1.595$, $P = 0.18$; ESD: $F = 1.057$, $P = 0.38$;

TABLE 1. Cell dimensions for different cell morphologies of the dinoflagellate *Ceratocorys horrida*. Values represent means ± standard errors of the means. Length, width, height, and spine length were based on stereomicroscope measurements of 20 cells of each morphology. Cell width and height were considered equal. See methods for a detailed description of equivalent spherical diameter and volume calculations. The proportion of vacuole volume to total volume was calculated based on measurements from confocal microscope images of luciferin fluorescence; n is the number of cells examined. N/P signifies that spines were not present.

Morphology	Length (μm)	Width and height (μm)	Equivalent spherical diameter (μm)	Total volume (μm^3)	Spine length (μm)	Proportion vacuole volume to total volume[a]
Long-spined	63.5 ± 1.5	52.9 ± 1.4	56.2	93,043	43.0 ± 0.6	0.28 ± 0.02[b] (n = 12)
Short-spined	48.2 ± 1.1	41.5 ± 0.8	43.6	43,396	22.0 ± 0.7	0.17 ± 0.02 (n = 11)
Spineless	40.5 ± 0.5	38.7 ± 0.6	39.25	31,660	N/P	0.14 ± 0.01 (n = 10)

[a] Values were significantly different (F = 23.899, df = 30, $P < 0.01$).
[b] Value significantly different from other cell types, Sheffe test, $P < 0.01$.

length: F = 1.209, P = 0.31; width: F = 1.365, P = 0.25; for all: df = 127). Once transformed, there was no significant change in the mean length of the antapical spines of short-spined cells with time of agitation (F = 1.850, df = 99, P = 0.13); after 4 mo of agitation, the length of the antapical spines was 19.9 ± 1.1 μm (n = 22). However, there was a significant decrease in the mean length of the dorsal and ventral spines with time of agitation (F = 10.634, df = 65, $P <$ 0.001) (Fig. 4). After 24 h to 4 mo of continuous agitation, only 30 to 40% of short-spined cells had measurable dorsal or ventral spines; the mean length of any dorsal and ventral spines that were still present was only 9.5 ± 1.1 μm (n = 10).

The loss or reduction of spines for agitated cells was not due to mechanical breakage. Scanning electron microscopy of these cells clearly showed no evidence of a fracture plane, which is visible when spines are broken off (e.g. Fig. 49H of Graham 1942). Furthermore, collisions due to cell swimming observed under the microscope did not result in cell damage or spine loss. The reduction or loss of spines most likely occurred through resorption of material as the endoskeleton was transformed.

TABLE 2. Net population growth rates of *Ceratocorys horrida* for different growth conditions at 20° C. Values represent the means ± standard errors of the means, with n representing the number of experiments. Doubling time was calculated from the growth rate for each experiment. Refer to text for details on methods. Spineless cells were individually isolated from agitated cultures and then monitored under still conditions.

Condition	n	Population growth	
		Growth rate (d^{-1})	Doubling time (d)
Still control	4	0.0580 ± 0.0150	15.04 ± 3.93
Agitated (75 rpm)	8	0.0059 ± 0.0103[a]	N/A
Recovery	4	−0.0057 ± 0.0037[a]	N/A
Recovery of spineless cells	9	0.0439 ± 0.0108	16.31 ± 3.90

[a] Value not significantly different from zero (agitated: t = 0.573, df = 7, $P > 0.05$; recovery: t = 1.532, df = 3, $P > 0.05$). N/A signifies not applicable because of negligible population growth rate.

Recovery under still conditions. The overall population growth rate of agitated cultures returned to still conditions and monitored for as long as 1 mo was not significantly different from zero (Table 2); however, there was a shift in population structure from short-spined to long-spined cells (Fig. 5). Over a period of 30 d, the rate of decrease in the abundance of short-spined cells (μ = −0.105 ± 0.008 d^{-1}; n = 4 experiments) was equivalent to the rate of increase in abundance of long-spined cells (μ = 0.108 ± 0.002 d^{-1}); the absolute values of these rates were not significantly different (t = 6.316, df = 6, P = 0.76), suggesting that short-spined cells were transforming into long-spined cells. During this time, the population growth rate of spineless cells (μ = 0.003 ± 0.005 d^{-1}) was not significantly different from zero (t = 0.617, df = 3, P = 0.58).

In a representative experiment, the transformation from short-spined to long-spined cells was apparent

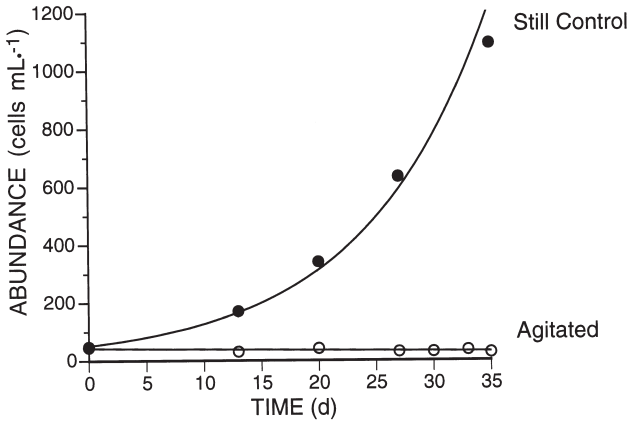

FIG. 2. Population growth of *Ceratocorys horrida* maintained under agitated (75 rpm shaking) and still conditions. In this representative experiment, at time zero two aliquots from the same culture were transferred into fresh medium. The curves represent least squares exponential regressions of cell abundance as a function of time. The aliquot grown under still conditions exhibited positive population growth (μ = 0.091 d^{-1}, doubling time = 7.6 d) and consisted of >99% long-spined cells, whereas that grown under agitated conditions exhibited a near-zero population growth rate (μ = −0.009 d^{-1}) and not all the cells were long-spined.

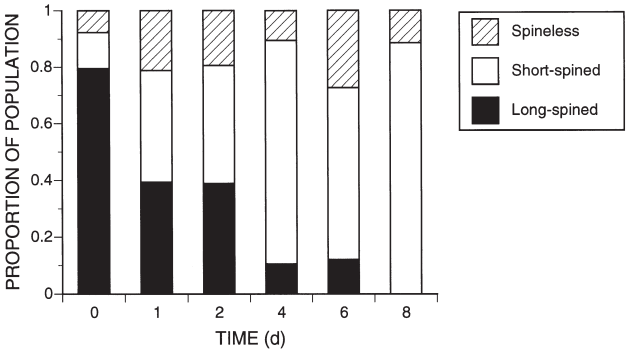

FIG. 3. Change in the population structure of *Ceratocorys horrida* cultures maintained under continuous agitation at 75 rpm. Cultures were subjected to active flow conditions starting on Day 0. Loss of long-spined cells from the population of agitated cells was complete after 8 d for this experiment.

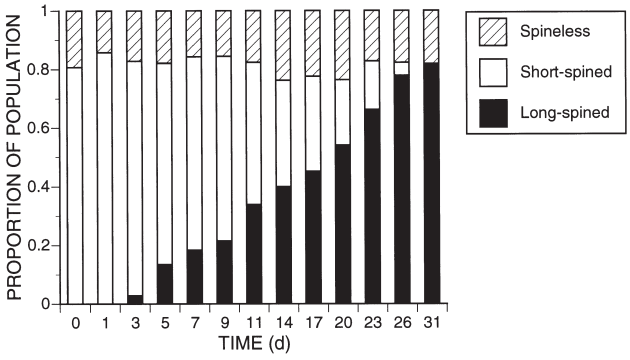

FIG. 5. Recovery in the population structure of *Ceratocorys horrida* for cultures that had been continuously agitated at 75 rpm for 17 d, and then returned to still conditions on Day 0. Data represent the mean values for 4 replicate cultures. Over the period of 30 d, even though the overall population growth rate was zero, the population structure shifted back to the long-spined cell type.

after several days (Fig. 5). After 1 d, approximately 10% of the population had begun to develop short dorsal and ventral spines <10 μm in length. Long-spined cells first reappeared at 3 d, when they comprised approximately 3% of the population; after two weeks, the population was composed of 40% long-spined cells, 36% short-spined cells, and 24% spineless cells. After 30 d, short-spined cells were no longer present in the population, which consisted of 82% long-spined cells and 18% small spineless cells. This population structure was similar to that of cultures maintained under still conditions.

Single-cell experiments confirmed that the elongation of the spines and the increase in cell size did not occur as a result of cell division. Spines on isolated short-spined cells grew in length from <10 μm to >30 μm in as little as 3 d, during which time no cells divided (Table 3). Daughter cells did not appear until after 6 d, at which point all observed cells were long spined. Therefore elongation of the spines occurred prior to cell division.

Spineless cells. In cultures maintained under still conditions, a small proportion of the population consisted of small thecate spineless cells. Spineless cells had a more angular shape, no spines, and undeveloped girdle and sulcal lists (Fig. 1). The wrinkled appearance of many spineless specimens prepared for SEM suggested that the thecae were thinner than for the other cell types. Cell volume was approximately one-third that of long-spined cells (Table 1). As stated above, the mean net growth rate of spineless cells in agitated populations ($\mu = 0.024 \pm 0.019$ d^{-1}) was not significantly different from zero ($t = 1.289$, df = 4, $P = 0.27$). In addition, there was no significant change in any measure of cell size of spineless cells even after 4 mo of agitation ($F \leq 2.867$, df = 10, $P > 0.10$ for all parameters). Even after 30 d of agitation, there was no significant change in the population proportion of small spineless cells. Not only was the proportion of spineless cells unchanged as a result of agitation, but

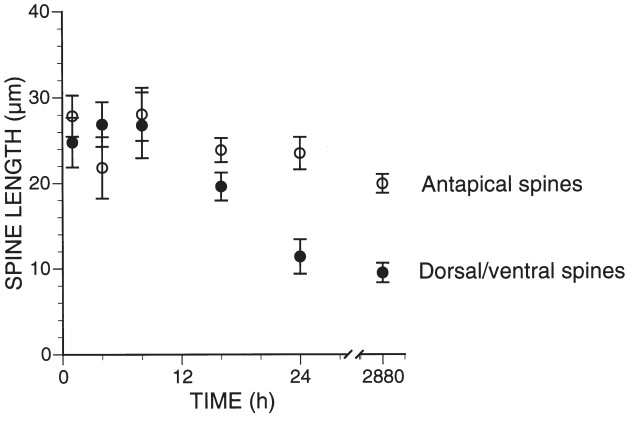

FIG. 4. Effect of continuous agitation at 75 rpm on the spine length of short-spined cells of *Ceratocorys horrida*. At each time point, the lengths of antapical spines from 12 to 30 cells, and dorsal or ventral spines of 9 to 25 cells were measured using a light microscope. There was a significant decrease in length of the dorsal or ventral spines, if present, with no significant change in the length of the antapical spines (see text for details).

TABLE 3. Recovery of single cells of *Ceratocorys horrida* under still conditions. Single short-spined cells from cultures agitated at 75 rpm were transferred to individual wells of a multiwell plate at day 0 and thereafter maintained under continuous illumination without agitation. Observations were made of *n* number of wells with observable cells out of an initial 15 wells. The proportion of dividing cells was based on the presence of multiple cells.

Day	*n*	Proportion long-spined cells	Proportion cells dividing
1	11	0	0
3	11	0.91	0
6	10	1.0	0.6
8	12	1.0	1.0

after return of agitated populations to still conditions there was no significant change in abundance of spineless cells (described in previous section).

These data suggest that spineless cells did not transform into long-spined or short-spined cells. To test this hypothesis directly, groups of spineless cells removed from an agitated population were resuspended in fresh medium and grown under still conditions. These cells exhibited a positive mean population growth rate ($\mu = 0.044 \pm 0.032\ d^{-1}$) significantly different from zero ($t = 4.06$, df = 8, $P < 0.05$). The appearance of other cell types after 1 d (Fig. 6) indicated that spineless cells were able to transform into both short-spined and long-spined cells.

Swimming and sinking. The swimming pattern of *C. horrida* consisted of the helical swimming path observed for other dinoflagellates (Kamykowski et al. 1992). Long-spined cells had a mean swimming speed of $4.4 \pm 0.6\ m \cdot d^{-1}$ ($n = 10$ cells) and a rotation rate of 15–30 rpm, similar to that of other dinoflagellates (Kamykowski et al. 1992). In the present study, a portion of the agitated population formed an accumulation of cells on the bottom of the flask, similar to that observed by White (1976) in agitated cultures of *Gonyaulax excavata* (= *Alexandrium tamarense*). Thomas and Gibson (1990a) observed that sheared cells of *Lingulodinium polyedrum* had reduced swimming ability, in their case due to loss of the longitudinal flagellum. The *C. horrida* cells that exhibited reduced swimming capability were not pellicle cysts, because they were observed to have thecae with spine rudiments. Up to 50% of the cells were observed intermittently swimming or rotating, suggesting that they possessed functional flagella.

According to Stokes' law, sinking rate is affected by cell size and cell density. To investigate whether morphological differences affected the sinking rate in *C. horrida*, nonswimming cells were videotaped while sinking. For each cell morphology, there was no significant difference in sinking rates for nicotine-narcotized and formaldehyde-treated cells (two-tailed *t*-test, $P > 0.05$). The sinking rate of long-spined cells was significantly less than that of short-spined cells (Table 4). Based on the results of sucrose density experiments, the density of short-spined cells was 1080 $kg \cdot m^{-}3$, similar to that of other dinoflagellates (Kamykowski et al. 1992), whereas long-spined cells had a density of 1160 $kg \cdot m^{-3}$. The larger, denser long-spined cells had a slower sinking rate than short-spined cells, counter to the prediction of Stokes' law for a simple spherical cell morphology.

Flow conditions in shaken flasks. To examine the effect of environmentally relevant levels of fluid motion, the flow field within shaken flasks was measured directly using DPIV and assessed using bioassays of population growth of the shear-sensitive dinoflagellate *L. polyedrum*. DPIV measurements of the flow in the flask yielded two dimensional mean velocities $\bar{u}$; and $\bar{v}$, and a mean shear stress map $\bar{\tau}$ (Fig. 7A) based on a 20 s average. Table 5 summarizes the mean velocities and shear stress values for three points A, B, and C positioned along the radius aligned with the *y*-axis of the flask. Along this radius, the mean velocities in the *y* direction, **v**, were approximately one order of magnitude lower than **u** and represented an approximate noise level of the velocity measurements. As expected, there was a region of enhanced shear along the wall (solid curved line) of the flask (Fig. 7A). For example, 2 mm from the wall (at point C) the mean shear stress was $0.00165\ N \cdot m^{-2}$ at 75 rpm. This shear layer near the wall was also apparent in the radial profiles of $\bar{u}(y)$ and $\bar{\tau}(y)$ (Fig. 7B and 7C, respectively). The flow in the shaken flask was unsteady with a periodic acceleration. For such pseudo-periodic signals, rms quantities yield valuable information about fluctuations in the flow field experienced by cells. For example, at point C, $u(t)$ was dominated by a 1.25 Hz (= 75 rpm) signal (Fig. 7D), the rms of the horizontal velocity was $u^{C}_{rms} = 0.6269\ cm \cdot s^{-1}$, and the rms of the shear stress was $\tau^{C}_{rms} = 0.0025\ N \cdot m^{-2}$ (Fig. 7E). If the

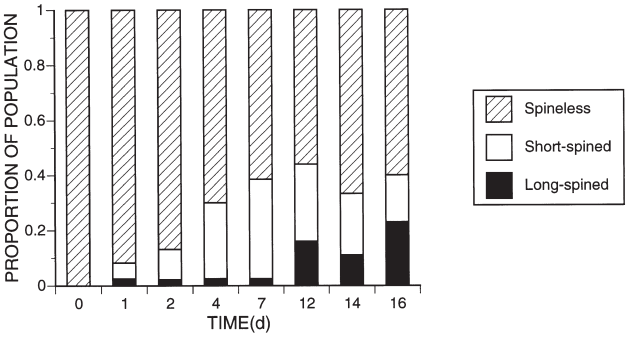

FIG. 6. Transformation of spineless cells of *Ceratocorys horrida* to other cell types upon return to still conditions. On Day 0, spineless cells isolated from a culture that had been agitated at 75 rpm for 10 d were placed in fresh medium and thereafter maintained under still conditions. After 16 d, the population consisted of 23% long-spined cells, 17% short-spined cells, and 60% spineless cells.

TABLE 4. Sinking rates of individual cells of *Ceratocorys horrida* measured for different cell types. Values represent the means ± standard errors of the means, with number of cells given as *N*. Refer to text for details on methods. Long-spined cells were grown under still conditions. Short-spined cells were maintained under continuous agitation at 75 rpm for 17 d.

	Sinking rate ($m \cdot d^{-1}$)[a]	
Morphology	Narcotized cells[b]	Fixed cells
Long-spined	24.2 ± 1.2 ($N = 28$)	23.9 ± 1.2 ($N = 13$)
Short-spined	29.7 ± 1.3 ($N = 20$)	29.3 ± 1.4 ($N = 13$)

[a] There was no significant difference between the sinking rates of nicotine-narcotized and formaldehyde-fixed cells within each morphology (long-spined: $t = 0.171$, $P = 0.865$; short-spined: $t = 0.179$, $P = 0.859$).

[b] Within each treatment, the sinking rate of short-spined cells was significantly different from that of long-spined cells (narcotized: $t = 3.027$, $P = 0.004$; fixed: $t = 2.973$, $P = 0.007$).

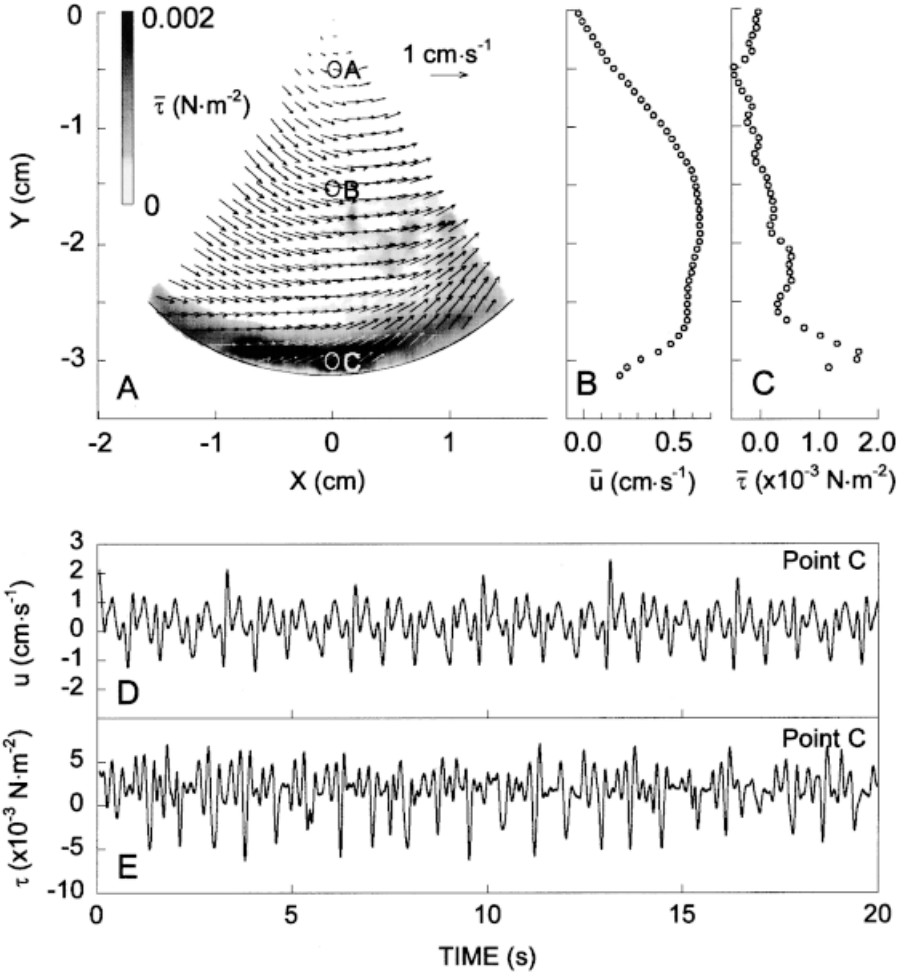

FIG. 7. Results of DPIV measurements of the flow field in the flask at 75 rpm. (A) 20 s average velocity and shear stress maps. For clarity, only 25% of the total velocity vectors are shown. Underlaid is the grayscale contour map of the mean shear stress. The velocity scale is given by the unit vector in the upper right corner and shear stress levels are represented on the grayscale bar. (B) Profile along the radius [AC] of the mean tangential velocity. (C) Profile along the radius [AC] of the mean shear stress. (D) 20 s time series of tangential velocity at 3 cm from the center of the flask (point C). (E) 20 s time series of shear stress at the same location.

characteristic shear stress value in the wall shear layer is between τ_{rms} and $\sqrt{2}\ \tau^{C}_{rms}$, then for the 75 rpm case the shear stress exerienced at a point near the wall was approximately 0.0025 to 0.0035 N·m^{-2}.

According to Couette flow studies of Thomas and Gibson (1990a), these levels of shear stress should reduce population growth in the dinoflagellate *L. polyedrum* (= *Gonyaulax polyedra*) to 18–61% of still control values as determined from cell counts. Tests verified that the flow conditions at a shaking rate of 75 rpm were sufficient to inhibit population growth of *L. polyedrum* compared with still controls ($t = 51.502$, df = 5, $P < 0.001$). The mean reduction in the growth rates of shaken populations to 38% of still control values is within the range predicted by Thomas and Gibson (1990a), based on the shear stress values obtained by DPIV.

The threshold level of agitation which caused a change in morphology in *C. horrida* occurred at 45 rpm. At this level of agitation, DPIV results indicated that the mean shear stress in the wall boundary layer was 0.000174 N·m^{-2} (Table 5), which is less than the threshold for the inhibition of population growth in *L. polyedrum* (Thomas and Gibson 1990a). As expected, growth studies with *L. polyedrum* at 45 rpm showed no significant difference between the rates of growth of shaken and still control populations ($t = 1.328$, df = 4, $P = 0.31$).

Populations of *C. horrida* were agitated at 120 rpm to determine the effect of higher rates of agitation on population growth and the rate of morphology transformation compared with that at the standard agitation condition at 75 rpm. Agitated populations exhibited negative growth indicating that cell mortality was occurring. Transformation of the population from full-spined to short-spined cells was completed in only 4 d. These data suggest that the rate of morphological transformation may be a function of agitation level. At an agitation rate of 120 rpm, DPIV measurements indicated that the mean shear stress in the boundary layer was 0.0055 N·m^{-2} (Table 5). However, this value is probably an underestimate of the actual shear stress in the boundary layer, because of appreciable fluid motion out of the plane of measurement at this rate of agitation.

DISCUSSION

Effect of flow on morphology. A wide variety of protozoan, plant, and animal cells respond to mechanical signals in their environment with morphological changes. Flow-induced cyclomorphosis is best known

TABLE 5. Summary statistics of DPIV measurements of fluid motion in the shaken flasks in a horizontal plane at half the fluid height. Fluid velocity in the x direction (**u**) and y direction (**v**), and shear stress, was calculated for three locations in the shaken flask corresponding to (A) 0.5 cm, (B) 1.5 cm, and (C) 3 cm from the center of the 6.2-cm-diameter flask. Values represent means ± standard errors of the mean.

Parameter	Location		
	A	B	C
1. 45 rpm			
u ($cm \cdot s^{-1}$)	0.020 ± 0.015	0.064 ± 0.013	0.028 ± 0.006
v ($cm \cdot s^{-1}$)	0.007 ± 0.025	0.019 ± 0.021	0.009 ± 0.010
Shear stress ($\times 10^{-3}$ $N \cdot m^{-2}$)	0.012 ± 0.028	0.019 ± 0.022	0.174 ± 0.033
2. 75 rpm			
u ($cm \cdot s^{-1}$)	0.250 ± 0.061	0.637 ± 0.060	0.244 ± 0.0361
v ($cm \cdot s^{-1}$)	0.065 ± 0.071	0.099 ± 0.060	0.099 ± 0.033
Shear stress ($\times 10^{-3}$ $N \cdot m^{-2}$)	0.453 ± 0.078	0.178 ± 0.072	1.652 ± 0.157
3. 120 rpm			
u ($cm \cdot s^{-1}$)	0.865 ± 0.207	2.421 ± 0.245	1.014 ± 0.168
v ($cm \cdot s^{-1}$)	−0.088 ± 0.175	0.076 ± 0.172	0.151 ± 0.099
Shear stress ($\times 10^{-3}$ $N \cdot m^{-2}$)	0.746 ± 0.412	0.288 ± 0.318	3.196 ± 1.413

in planktonic freshwater cladocerans such as *Daphnia* (Brooks 1947, Hrbácek 1959, Havel and Dodson 1985), although the morphologies of field populations represent the response to a suite of environmental factors, including the presence of predators. Hydrodynamic conditions also affect the morphology of benthic organisms such as seaweeds (Armstrong 1989, Blanchette 1997), foraminifera (Khare et al. 1995), diatoms (Gomez et al. 1995), and bivalves (Hinch et al. 1986, Bailey and Green 1988). Flow-induced morphological changes have been described in nonmarine organisms such as bacteria, yeast, filamentous molds, and mammalian cells (Wase and Patel 1985, Edwards et al. 1989, Davies and Dull 1990), and some terrestrial plants are known to morphologically change in response to mechanical stimuli from wind and touch (Braam 1993).

In the present study using carefully controlled experimental conditions, fluid motion equivalent to that caused by light wind and waves at the sea surface caused a change in population structure of *C. horrida* in the absence of net positive population growth. Initially long-spined cells transformed into a short-spined cell type, such that after 8 to 12 d at 20° C long-spined cells had disappeared from the population. The short-spined cell type has never been previously observed in laboratory cultures of *C. horrida*. The morphological change due to fluid motion was completely reversible. Upon return to still conditions, short-spined cells gradually disappeared from the population until it was once again dominated by long-spined cells. Therefore, the hypothesis that the transformation in cell morphology was due solely to fluid motion is supported. Changes in the abundance of long-spined and short-spined cells of *C. horrida* always mirrored each other. In addition, single-cell studies demonstrated that cells regrew spines prior to cell division. Therefore, based on growth rate and cell morphology data the hypothesis that the transformation in cell morphology occurs as a result of cell division must be rejected.

Flow-induced changes in morphology of *C. horrida* under conditions of inhibited population growth were different from the enlarged cells and increased mortality observed in other dinoflagellates at higher levels of agitation (Pollingher and Zemel 1981, Berdalet 1992, Thomas et al. 1995). In the present study of *C. horrida*, gentle agitation maintained for periods > 30 d did not result in cell death, nor were enlarged cells ever observed. Although no net population growth occurred, cells remained viable, pigmented, and flagellated. Once the population structure had shifted toward short-spined cells, there was no further change in cell morphology or population dynamics.

Some dinoflagellates are known to shed their thecae and flagella under adverse environmental conditions and form a pellicle cyst (Schmitter 1979, Marasovic 1989) in order to temporarily escape hazardous conditions (Kofoid 1908). In neither the present nor previous studies (Thomas and Gibson 1990a, Berdalet 1992) have agitated flow conditions, sufficient to inhibit dinoflagellate population growth, resulted in formation of pellicle cysts.

Spineless cells. Small spineless cells accounted for approximately 20% or less of the population under all experimental conditions. The spineless cells may be similar to small cells known to occur for other dinoflagellate species (Silva and Faust 1995). However, unlike small cells for other species, the small cells of *C. horrida* had a different morphology from the typical long-spined cells. The small cells were thecate, flagellated, and motile but devoid of spines and wide girdle

and sulcal lists present in cells of the long-spined and short-spined cell types. The volume of small spineless cells was 0.34 times that of long-spined cells, within the range of 0.16–0.5 found in other dinoflagellate species (Silva and Faust 1995). Furthermore, the relative size of the vacuole was reduced by one-half relative to the typical long-spined cell type.

The occurrence of small spineless cells did not appear to be related to population growth rate. Small cells constituted a nearly constant proportion of the population under still conditions when populations were experiencing maximum exponential growth, as well as during periods of agitation and the recovery from agitation when population growth rates were approximately zero. Even though the abundance of spineless cells did not change, single-cell studies indicated that the spineless cells were able to transform rapidly into long-spined and short-spined cells in the absence of cell division.

The thecal plates of spineless cells observed with SEM appeared to be thinner than those of the other cell types of *C. horrida*, although plate thickness was not measured in the present study. Graham (1942) described a similar type of cell of *C. horrida* from the Carnegie collection that was spineless, with undeveloped girdle and sulcal lists and thin wall, suggesting that it was recently formed. Graham concluded that this cell type originated through ecdysis and subsequent formation of all thecal plates. Buchanan (1968) described a similar cell type for the dinoflagellate *Pyrodinium bahamense*, characterized by thin, undeveloped thecal plates and the absence of lists. He considered this cell type, which he called the thecal development stage, to be a transition between an athecate gymnodinoid stage and the typical thecate cell type. If the spineless cells of *C. horrida* observed in the present study are recently formed, then they did not originate via the conventional mode of cell division in which the original thecal plates are shared between daughter cells (described in the next section). In addition, the absence of pellicle or thick-walled cysts from control or agitated populations suggests that excystment was not a likely mechanism in this oligotrophic oceanic species. *C. horrida* may possess an as yet undescribed life cycle stage, perhaps involving a sexual phase, which results in the complete formation of new thecae.

Morphological variability. Although the plate pattern of *C. horrida* specimens represented in plankton collections is quite constant, considerable morphological variability has been observed in thecal wall thickness, spine thickness and length, cell size, and general body ornamentation (Kofoid 1910, Graham 1942). The flow-induced changes in morphology observed in the present study were not consistent with a mechanism based on cell division, in which the left daughter cell receives the dorsal and ventral spines and reforms the four antapical spines and the right daughter cell receives the four antapical spines and reforms the dorsal and ventral spines (Kofoid 1910, Graham 1942, Taylor 1976) (Fig. 8).

Spines of *C. horrida* have been reported to range from 60 μm to > 120 μm in length (Graham 1942, Balech 1949, Taylor 1976). The Carnegie collection contains cells with short spines (Fig. 49D of Graham 1942), similar to the short-spined cells induced by agitation in the present study. In addition, one Carnegie specimen of *C. horrida* is depicted as completely spineless, with undeveloped lists and a thin wall (Fig. 50 of Graham 1942). Even though the size of this cell is typical of spined cells, its thecal plate and list morphologies are similar to those of the small spineless cells observed in the present study. These similarities suggest that the cell morphologies observed in laboratory cultures may occur in natural populations.

Agitation and turbulence. It is virtually impossible to recreate oceanic turbulence in the laboratory. As discussed by Peters and Redondo (1997), laboratory flow

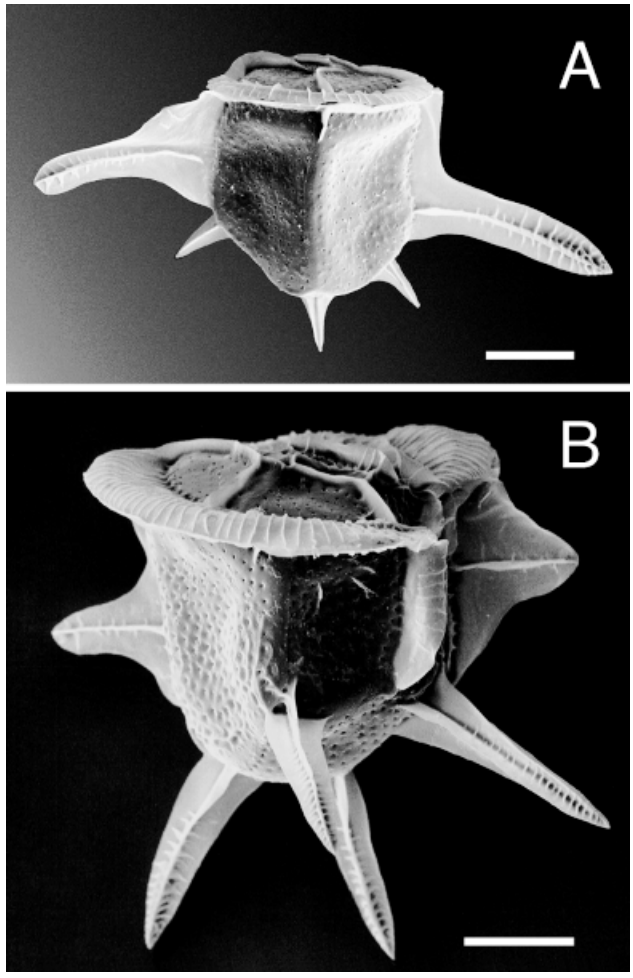

FIG. 8. Effect of cell division on the morphology of *Ceratocorys horrida*. Cells maintained under still conditions were prepared for SEM. Scale bars represent 20 μm. (A) Dorsal view of a left daughter cell, which has received the dorsal and ventral spines. The cell is regrowing the apical spines, three of which are visible. (B) Ventral view of a right daughter cell, which has received the four antapical spines and is in the process of regrowing the dorsal and ventral spines.

fields generate turbulence levels that are generally higher than *in situ* values because of differences in the integral length scales, and they do not approximate the temporal intermittency of small-scale shear in oceanic turbulence. Each laboratory flow field chosen has limitations (Peters and Redondo 1997). The present study used shaken flasks to create an agitated condition, as have many other studies on the effect of water motion on phytoplankton (e.g. Tuttle and Loeblich 1976, White 1976, Pollingher and Zemel 1981, Berdalet 1992). Although flow velocity in shaken flasks has been measured (e.g. Pearson et al. 1998), this is to our knowledge the first study to quantify fluid motion in terms of shear stress.

Because flow-induced effects on dinoflagellates appear to be mediated through fluid shear (Thomas and Gibson 1990a, 1992, Latz et al. 1994, Latz and Rohr 1999), boundary layer shear conditions in the shaken flasks should be most important in determining how cells respond to fluid motion. The present DPIV measurements of flow in a horizontal plane through the midsection of the fluid volume encompassed the flask side wall boundary layer, where shear levels are expected to be highest. The bottom boundary layer, while not studied by DPIV, should contain shear levels that depend on radial position but are equal to or less than that at the wall.

Both DPIV and bioassays using the dinoflagellate *L. polyedrum* provided a consistent characterization of the flow conditions within the agitated flasks. At the standard oscillation rate of 75 rpm, levels of shear stress in the flask wall boundary layer were approximately 0.0025 to 0.0035 $N \cdot m^{-2}$. The measured amount of inhibition of population growth of *L. polyedrum* at this agitation rate was consistent with the predictions of Thomas and Gibson (1990a) based on Couette flow studies. Similarly, a mean boundary layer shear stress value of 0.000174 $N \cdot m^{-2}$ at 45 rpm, the threshold for morphological transformation in *C. horrida*, did not cause inhibition of population growth in *L. polyedrum*, as predicted by Thomas and Gibson (1990a). Therefore levels of boundary layer shear stress as measured by DPIV appear to represent accurately the mean shear experienced by cells in the agitated flasks as determined by population growth bioassays.

The DPIV measurements also indicate that the previously uncharacterized flow field in shaken flasks can be directly related to defined laboratory flow fields, such as Couette flow. For example, studies of population growth of *L. polyedrum* using both shaken flasks and quantified Couette shear flow indicate similar effects, depending on the time during the photoperiod during which agitation is applied (Juhl 1998). In addition, the growth of natural populations of the dinoflagellate *Peridinium gatunense*, which is inhibited by nighttime but not daytime winds, is mirrored in laboratory studies where the shaking of culture flasks inhibits population growth when applied during the night phase but not the day phase (Pollingher and Zemel 1981). Although laboratory flow fields do not recreate the proper scales of oceanic turbulence, they are useful tools for testing the physiological and behavioral effects of fluid motion. Turbulent eddy length and time scales as well as their intermittency need to be adequately described at the small scales appropriate for dinoflagellates, especially in the upper 0–10 m of the water column, where dinoflagellate blooms often accumulate. Until then, laboratory flow fields are the best way to study the effects of water motion on plankton and to identify physiological mechanisms underlying such effects.

Bearing in mind the limitations of laboratory conditions to describe ocean flows, it is still possible to compare the shear stresses created in the laboratory with those found in the ocean. Historically, turbulent flows in the ocean have been characterized by the rate of kinetic energy dissipation ε (reviewed by Gargett 1989). However, for isotropic turbulence the shear strain and dissipation rate are related by (Tennekes and Lumley 1972)

$$\varepsilon = \frac{15\ \mu_{\text{seawater}}}{2\ \rho_{\text{seawater}}}\overline{\left(\frac{\partial u}{\partial y}\right)^2}$$

Hence, a shear stress on the order of 0.002 to 0.004 $N \cdot m^{-2}$ yields an associated value of order of 10^{-5} to 10^{-4} $m^2 \cdot s^{-3}$ for the dissipation rate. Such values might be considerably larger than those found at depth in the ocean (e.g. Fig. 1 of Moum et al. 1995) but are consistent with those found in the upper mixed layer or surface-wave zone. In fact, Veron and Melville (1999) found $\varepsilon = 10^{-5}$ $m^2 \cdot s^{-3}$ for a wind speed of 6.7 $m \cdot s^{-1}$ at a depth of 50 cm and $\varepsilon = 10^{-4}$ $m^2 \cdot s^{-3}$ for a wind speed of 10.3 $m \cdot s^{-1}$ at a depth of 50 cm. These values also compared favorably with those reported by Drennan et al. (1996), $\varepsilon \approx 2 \times 10^{-4}$ $m^2 \cdot s^{-3}$ for a depth of 1.25 m and a wind speed of 12 $m \cdot s^{-1}$, and by Anis and Moum (1995), who found $\varepsilon \approx 3 \times 10^{-4}$ $m^2 \cdot s^{-3}$ for a depth of 1.5 to 5 m and a wind speed of 13 $m \cdot s^{-1}$. Thus, the levels of shear stress generated in the shaken flask at 75 rpm are comparable to those associated with turbulent flow in the first few meters of the ocean under calm to moderate wind and wave conditions.

Ecological significance of the morphology change. The functional significance of the unique and elaborate forms of dinoflagellates has been widely discussed (e.g. Sournia 1982). Environmental factors hypothesized to affect dinoflagellate cell morphology include nutrient conditions (Peters 1934, Margalef 1997) and water temperature (Dowidar 1972). Chemical signals from predators are known to lead to inducible changes in the morphology of cladocerans (reviewed by Havel 1987) and a chlorophyte (Lürling 1998), attesting to the importance of morphological specializations as an antipredation strategy. The present study is the first demonstration that the length and number of dinoflagellate spines can be modified by hydrodynamic conditions.

Morphological adaptations such as spines and horns may act to reduce grazing on cells, but they can also increase form drag and reduce the rate of cell sinking (Walsby and Xypolyta 1977, Takahashi and Allan 1984, Alexander 1990). The flow-induced reduction of spine length in *C. horrida* cells resulted in a significant increase in sinking rate compared with long-spined cells, even though short-spined cells were smaller in size and had a lower cell density. Stokes' law predicts that spherical cells with the same size and density of long-spined cells of *C. horrida* would have a sinking rate four times greater than that of smaller and less dense short-spined cells. These results suggest that the reduction in sinking rate of long-spined cells occurs through an increase in form resistance due to drag by the spines, despite an increase in cell density due to the presence of the spines. Actual *in situ* vertical displacement of *C. horrida* cells would be a function not only of sinking, but also of fluid mixing and transport, and cell swimming. If oceanic turbulence inhibits dinoflagellate cell swimming, as suggested by laboratory experiments (Pollingher and Zemel 1981, Thomas and Gibson 1990a, present study), then cells may sink from near-surface turbulent layers into more quiescent deeper water. Thus a behavioral response in the form of reduced swimming may be an important short-term effect of turbulence, although under certain conditions turbulent water motion may overwhelm cell swimming or sinking (Kamykowski et al. 1988).

The ecological role of the morphological change in *C. horrida* due to agitation may be to allow cells to avoid near-surface regions of high shear, which inhibit population growth. As a result of the transformation in morphology, which results in smaller short-spined cells with a higher sinking rate along with a reduction in swimming speed, cells will move away from high-shear surface waters into more quiescent conditions where they can return to the long-spined morphology and resume cell division. For flow conditions with mean shear stress values of 0.002 to 0.004 $N \cdot m^{-2}$, the morphology and swimming changes were initiated within 1 h and were complete after 8 d of continuous agitation. Temperatures higher than 20° C, known to be at the low end of the range for *C. horrida* (Graham 1942), may increase the rate at which the morphological changes occur. In addition, at higher levels of agitation the transformation to short-spined cells occurred faster than at 75 rpm and cell mortality occurred. Thus, actual *in situ* population structure at any particular time may be expected to represent a dynamic equilibrium reflecting recent hydrodynamic, temperature, and possibly other environmental conditions.

C. horrida appears to be one of the most shear-sensitive organisms known. The threshold for morphological change occurred at shear stress levels approximately one order of magnitude less than that inhibiting population growth in the well-studied dinoflagellate *L. polyedrum* (Thomas and Gibson 1990a). The response threshold for flow-induced bioluminescence in *C. horrida* is also less than that for other luminescent dinoflagellate species, including *L. polyedrum* (Nauen 1998). Perhaps the long spines of *C. horrida* act as levers to accentuate the effect of shear across the cell surface. The ability to rapidly and reversibly modify cell morphology in response to oceanic flow conditions may be an important ecological survival strategy for *C. horrida* and possibly other planktonic organisms.

We are grateful to A. Juhl, R. Kaufman, J. Nauen, and S. Rapoport for technical assistance, to C. Graham of the SIO Analytical Facility for assistance with SEM, to K. Melville for use of the DPIV apparatus, and to J. Price and the NSF–Whitaker Quantitative Microscopy and Confocal Imaging Resource in the Institute for Biomedical Engineering for assistance with confocal microscopy. A. Juhl, S. Lindsay, J. Nauen, and P. von Dassow provided useful comments on the manuscript. Supported by grant N00014-95-1-0001 from the Office of Naval Research (to MIL).

Alexander, R. M. 1990. Size, speed and buoyancy adaptations in aquatic animals. *Amer. Zool.* 30:189–96.

Anis, A. & Moum, J. N. 1995. Surface wave–turbulence interactions: scaling $\epsilon(z)$ near the sea surface. *J. Phys. Oceanogr.* 25: 346–66.

Armstrong, S. L. 1989. The behavior in flow of the morphologically variable seaweed *Hedophyllum sessile* (C. Ag.) Setchell. *Hydrobiologia* 183:115–22.

Bailey, R. C. & Green, R. H. 1988. Within-basin variation in the shell morphology and growth rate of a freshwater mussel. *Can. J. Zool.* 66:1704–8.

Balech, E. 1949. Estudio de *Ceratocorys horrida* Stein var. *extensa* Pavillard. *Physis* 20:166–73.

Berdalet, E. & Estrada, M. 1993. Effects of turbulence on several dinoflagellate species. *In* Smayda, T. J. & Shimizu, Y. [Eds.] *Toxic Phytoplankton Blooms in the Sea.* Elsevier Science Publishers B.V., Amsterdam, pp. 737–40.

Berdalet, E. 1992. Effects of turbulence on the marine dinoflagellate *Gymnodinium nelsonii*. *J. Phycol.* 28:267–72.

Blanchette, C. A. 1997. Size and survival of intertidal plants in response to wave action: a case study with *Fucus gardneri*. *Ecology* 78:1563–78.

Braam, J. 1993. 12. Developmental and molecular responses to touch in plants. *In* Spradling, A. C. [Ed.] *Evolutionary Conservation of Developmental Mechanisms.* Wiley-Liss, New York, pp. 185–98.

Brooks, J. L. 1947. Turbulence as an environmental determinant of relative growth in *Daphnia*. *Proc. Natl. Acad. Sci. USA* 33:141–8.

Buchanan, R. J. 1968. Studies at Oyster Bay in Jamaica, West Indies. IV. Observations on the morphology and asexual cycle of *Pyrodinium bahamense* Plate. *J. Phycol.* 4:272–7.

Costas, E., Fernandez, J. L., Navarro, M. & Varela, M. 1988. A comparative morphometrical study of the ultrastructural organization in six dinoflagellate species using stereology. *Bot. Mar.* 31:555–62.

Cowles, T. J. & Desiderio, R. A. 1993. Resolution of biological microstructure through *in situ* fluorescence emission spectra: an oceanographic application using optical fibers. *Oceanography* 6:105–11.

Davies, P. F. & Dull, R. O. 1990. How does the arterial endothelium sense flow? Hemodynamic forces and signal transduction. *Adv. Exp. Med. Biol.* 273:281–93.

Denman, K. L. & Gargett, A. E. 1983. Time and space scales of vertical mixing and advection of phytoplankton in the upper ocean. *Limnol. Oceanogr.* 28:801–15.

Dowidar, N. M. 1972. Morphological variations in *Ceratium egyptiacum* in different natural habitats. *Mar. Biol.* 16:138–49.

Drennan, W. M., Donelan, M. A., Terray, E. A. & Katsaros, K. B. 1996. Oceanic turbulence dissipation measurements in SWADE. *J. Phys. Oceanogr.* 26:808–15.

Eckert, R. & Reynolds, G. T. 1967. The subcellular origin of bioluminescence in *Noctiluca miliaris*. *J. Gen. Physiol.* 50:1429–54.

Edwards, N., Beeton, S., Bull, A. T. & Merchuk, J. C. 1989. A novel device for the assessment of shear effects on suspended microbial cultures. *Appl. Microbiol. Biotechnol.* 30:190–5.

Estrada, M. & Berdalet, E. 1997. Phytoplankton in a turbulent world. *Sci. Mar.* 61(Suppl. 1):125–40.
Fenchel, T. 1988. Marine plankton food chains. *Annu. Rev. Ecol. Syst.* 19:19–38.
Gargett, A. E. 1989. Ocean turbulence. *Annu. Rev. Fluid Mech.* 21:419–51.
Gomez, N., Riera, J. L. & Sabater, S. 1995. Ecology and morphological variability of *Aulacoseira granulata* (Bacillariophyceae) in Spanish reservoirs. *J. Plankton Res.* 17:1–16.
Graham, H. W. 1942. Studies in the morphology, taxonomy, and ecology of the Peridiniales. *Sci. Results Cruise VII Carnegie Biol. Ser.* 3:1–129.
Havel, J. E. 1987. Predator-induced defenses: a review. *In* Kerfoot, W. C. & Sih, A. [Eds.] *Predation: Direct and Indirect Impacts on Aquatic Communities.* University Press of New England, Hanover, New Hampshire, pp. 263–78.
Havel, J. E. & Dodson, S. I. 1985. Environmental cues for cyclomorphosis in *Daphnia retrocurva* Forbes. *Freshwater Biol.* 15:469–78.
Hinch, S. G., Bailey, R. C. & Green, R. H. 1986. Growth of *Lampsilis radiata* (Bivalvia: Unionidae) in sand and mud: a reciprocal transplant experiment. *Can. J. Fish. Aquat. Sci.* 43:548–52.
Hrbácek, J. 1959. Circulation of water as a main factor influencing the development of helmets in *Daphnia cucullata* Sars. *Hydrobiologia* 13:170–85.
Juhl, A. R. 1998. The effect of turbulence on growth of a red-tide dinoflagellate. *Eos* 79:OS9.
Kamykowski, D., McCollum, S. A. & Kirkpatrick, G. J. 1988. Observations and a model concerning the translational velocity of a photosynthetic marine dinoflagellate under variable environmental conditions. *Limnol. Oceanogr.* 33:66–78.
Kamykowski, D., Reed, R. E. & Kirkpatrick, G. J. 1992. Comparison of sinking velocity, swimming velocity, rotation and path characteristics among six marine dinoflagellate species. *Mar. Biol.* 113:319–28.
Karp-Boss, L., Boss, E. & Jumars, P. A. 1996. Nutrient fluxes to planktonic osmotrophs in the presence of fluid motion. *Oceanogr. Mar. Biol. Annu. Rev.* 34:71–107.
Khare, N., Sinha, R., Rai, A. K. & Nigam, R. 1995. Distributional pattern of benthic foraminiferal morpho-groups in the shelf region off Mangalore: environmental implications. *Indian J. Mar. Sci.* 24:162–5.
Kiørboe, T. 1993. Turbulence, phytoplankton cell size, and the structure of pelagic food webs. *Adv. Mar. Biol.* 29:1–72.
Kofoid, C. A. 1908. Exuviation, autotomy, and regeneration in *Ceratium. Univ. Calif. Publ. Zool.* 4:345–86.
Kofoid, C. A. 1910. A revision of the genus *Ceratocorys*, based on skeletal morphology. *Univ. Calif. Publ. Zool.* 6:177–87.
Latz, M. I. & Lee, A. O. 1995. Spontaneous and stimulated bioluminescence in the dinoflagellate, *Ceratocorys horrida* (Peridiniales). *J. Phycol.* 31:120–32.
Latz, M. I. & Rohr, J. 1999. Luminescent response of the red tide dinoflagellate *Lingulodinium polyedrum* laminar and turbulent flow. *Limnol. Oceanogr.* 44:1423–35.
Latz, M. I., Case, J. F. & Gran, R. L. 1994. Excitation of bioluminescence by laminar fluid shear associated with simple Couette flow. *Limnol. Oceanogr.* 39:1424–39.
Lazier, J. R. N. & Mann, K. H. 1989. Turbulence and the diffusive layers around small organisms. *Deep-Sea Res.* 36:1721–33.
Lürling, M. 1998. Effect of grazing-associated infochemicals on growth and morphological development in *Scenedesmus acutus* (Chlorophyceae). *J. Phycol.* 34:578–86.
Marasovic, I. 1989. Encystment and excystment of *Gonyaulax polyedra* during a red tide. *Estuarine Coastal Shelf Sci.* 28:35–41.
Margalef, R. 1997. Turbulence and marine life. *Sci. Mar.* 61(Suppl. 1):109–23.
Melville, W. K., Shear, R. & Veron, F. 1998. Laboratory measurements of the generation and evolution of Langmuir circulations. *J. Fluid Mech.* 364:31–58.
Moum, J. N., Gregg, M. C., Lien, R. C. & Carr, M. E. 1995. Comparison of turbulence kinetic energy dissipation rate estimates from two ocean microstructure profilers. *J. Atmos. Ocean Technol.* 12:346–66.
Nauen, J. C. 1998. Biomechanics of two aquatic defense systems. 1. The scaling of tail-flip kinematics and force production by the California spiny lobster *Panulirus interruptus*. 2. Shear sensitivity and interspecific variation in flow-stimulated dinoflagellate bioluminescence. Ph.D. Dissertation, University of California San Diego, 150 pp.
Netzel, H. & Dürr, G. 1984. Dinoflagellate cell cortex. *In* Spector, D. L. [Ed.] *Dinoflagellates.* Academic Press, Orlando, Florida, pp. 43–105.
Pasciak, W. J. & Gavis, J. 1975. Transport limited nutrient uptake rates in *Ditylum brightwellii*. *Limnol. Oceanogr.* 20:604–17.
Pearson, G. A., E. A. Serrao & S. H. Brawley. 1998. Control of gamete release in fucoid algae: sensing hydrodynamic conditions via carbon acquisition. *Ecology* 79:1725–39.
Peters, N. 1934. Die Bevölkerung des sudatlantischen Ozeans mit Ceratien. *Wiss. Ergebn. Dtsch. Atlant. Exped. "Meteor"* 12:1–69.
Peters, F. & Redondo, J. M. 1997. Turbulence generation and measurement: application to studies on plankton. *Sci. Mar.* 61(Suppl. 1):205–28.
Pollingher, U. & Zemel, E. 1981. *In situ* and experimental evidence of the influence of turbulence on cell division processes of *Peridinium cinctum* forma *westii* (Lemm.) Lefèvre. *Br. Phycol. J.* 16:281–7.
Rapoport, H. S. & Latz, M. I. 1998. *In situ* bioluminescence measurements from the Scripps Pier, La Jolla, California. *Eos* 79(1):OS25.
Schmitter, R. E. 1979. Temporary cysts of *Gonyaulax excavata*: effects of temperature and light. *In* Taylor, D. L. & Seliger, H. H. [Eds.] *Toxic Dinoflagellate Blooms.* Elsevier North Holland, New York, pp. 123–6.
Silva, E. S. & Faust, M. A. 1995. Small cells in the life history of dinoflagellates (Dinophyceae): a review. *Phycologia* 34:396–408.
Sournia, A. 1982. Form and function in marine phytoplankton. *Biol. Rev. Camb. Philos. Soc.* 57:347–94.
Takahashi, K. & Allan, W. H. 1984. Planktonic foraminifera: factors controlling sinking speeds. *Deep-Sea Res.* 31:1477–500.
Taylor, F. J. R. 1976. Dinoflagellates from the International Indian Ocean Expedition. A report on material collected by the R.V. "Anton Bruun" 1963–1964. *Bibl. Bot.* 132:1–234.
Tennekes, H., & Lumley, J. L. 1972. *A first course in turbulence.* MIT Press, Cambridge, Massachusetts, 300 pp.
Thomas, W. H. & Gibson, C. H. 1990a. Quantified small-scale turbulence inhibits a red tide dinoflagellate, *Gonyaulax polyedra* Stein. *Deep-Sea Res.* 37(10):1583–93.
Thomas, W. H. & Gibson, C. H. 1990b. Effects of small-scale turbulence on microalgae. *J. Appl. Phycol.* 2:71–7.
Thomas, W. H. & Gibson, C. H. 1992. Effects of quantified small-scale turbulence on the dinoflagellate *Gymnodinium sanguineum* (*splendens*): contrasts with *Gonyaulax* (*Lingulodinium*) *polyedra*, and the fishery implication. *Deep-Sea Res.* 39:1429–37.
Thomas, W. H., Vernet, M. & Gibson, C. H. 1995. Effects of small-scale turbulence on photosynthesis, pigmentation, cell division, and cell size in the marine dinoflagellate *Gonyaulax polyedra* (Dinophyceae). *J. Phycol.* 31:50–9.
Tuttle, R. C. & Loeblich, A. R., III. 1976. An optimal growth medium for the dinoflagellate *Cryptothecodinium cohnii*. *Phycologia* 14:1–8.
Tynan, C. T. 1993. The effects of small-scale turbulence on dinoflagellates. Ph.D. Dissertation, University of California, San Diego, 227 pp.
Veron, F. & Melville, W. K. 1999. Pulse-to-pulse coherent Doppler measurements of waves and turbulence. *J. Atmos. Ocean Technol.* 16:1580–97.
Vogel, S. 1994. *Life in Moving Fluids.* 2nd ed. Princeton University Press, Princeton, New Jersey, 467 pp.
Walsby, A. E. & Xypolyta, A. 1977. The form resistance of chitan fibres attached to the cells of *Thalassiosira fluviatilis* Hustedt. *Br. Phycol. J.* 12:215–23.
Wase, D. A. & Patel, Y. R. 1985. Variations in the volumes of microbial cells with change in the agitation rates of chemostat cultures. *J. Gen. Microbiol.* 131:725–36.
White, A. W. 1976. Growth inhibition caused by turbulence in the toxic marine dinoflagellate *Gonyaulax excavata*. *J. Fish. Res. Bd. Canada* 33:2598–602.
Willert, C. E., & Gharib, M. 1991. Digital particle image velocimeter. *Exp. Fluids* 10:181–93.